

## Compact Waterjets for High-Speed Ships

David R. Lavis<sup>1</sup>, [david.lavis@cdicorp.com](mailto:david.lavis@cdicorp.com)  
Brian G. Forstell<sup>1</sup>, [brian.forstell@cdicorp.com](mailto:brian.forstell@cdicorp.com)  
John G. Purnell<sup>1</sup>, [john.purnell@cdicorp.com](mailto:john.purnell@cdicorp.com)

### Abstract

*The paper describes the development and validation of a compact waterjet propulsion system for high-speed vessels. The development was conducted in four discrete phases over a period of 4 years: **Phase 1** studied pump-type options for compact units, **Phase 2** used advanced Computational Fluid Dynamics (CFD) to design the preferred pump type for a high-speed ship design, **Phase 3** involved the manufacture and performance/cavitation testing of a model of the pump designed in Phase 2, and **Phase 4** involved the construction and testing, in a towing tank, of a self-propelled model to determine the critical interaction effects between the hull and the waterjet inlet.*

*Following an introduction that serves to define the challenge, the paper discusses what is good and not so good about marine waterjet propulsion. The paper then describes the design approach, the design tools used, the testing procedures and the validation comparison of CFD predicted and model test results. The paper also describes the whole-ship impact of using these advanced pumps in terms of the significant improvements possible in ship speed, range or payload.*

*The overall program was considered to be an outstanding success with the potential of having major benefits to future high-speed ships.*



*19.8-foot self-propelled model*

### Key Words

*Waterjet; Propulsion; High-Speed Vessels; Computational Fluid Dynamics; Cavitation; Model Tests*

---

<sup>1</sup> CDI Marine Systems Development Division (CDIM-SDD) (formerly Band, Lavis & Associates, Inc.)

## 1. Introduction

To first put the ship propulsion challenge into context, Figure 1 has been included to define the overall propulsion powering demand for surface ships. It is based on the Circle Q and K relationships made famous by Froude in the mid to late 1800's. It compares Transport Factor ( $WV/P = 1/\text{CircleQ}$ ) versus non-dimensional ship speed and shows this for a very wide range of vessel types from monohulls to multihulls, SWATH, hydrofoils, SES, ACV's and hydroplanes. The challenge is that as speed increases, the Transport Factor falls off rapidly. This is due to a number of reasons. The main reason, of course, is the rapid increase in drag. Over the years, this has been overcome primarily by disconnecting the vessel from the water. As we see in Figure 1, these attempts have been reasonably successful, with hydrofoils, SES, ACV's and hydroplanes occupying the best positions on the right-hand side of the chart.

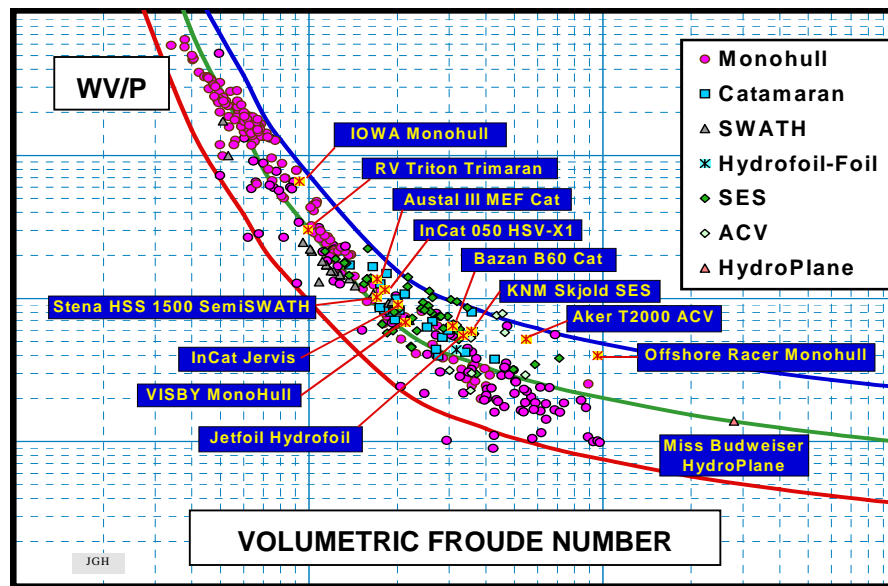


Figure 1: The overall powering challenge for surface ships  
(Based on an expansion of data from *Hoyt (2002)*)

However, as we decouple from the water, so we find it harder to find efficient propulsion devices to do an adequate job. Thus, Figure 1 represents the various attempts to head off this challenge of the huge increase in power with increasing speed and decreasing Transport Factor. For large high-speed ships, there is not much chance to fly, so the current push is to reduce drag using slender hulls and to eliminate appendage drag by using surface drives or waterjets with flush inlets. However, the more slender the hull, the tougher it is to accommodate the propulsion units, which is the challenge and subject of the work described in this paper.

### 1.1. So Why Marine Waterjet Propulsion?

It is evident that today there is a growing worldwide interest in high-speed ships for which waterjet propulsion is the popular choice. Within the U.S. Armed Forces, the Navy, the Marines and the Army are now all interested in fast waterjet-propelled vessels. This is because by comparison to marine screws, waterjet propulsion systems, with inlets mounted flush with the hull, have no appendage drag and have low navigational draft and low vulnerability to damage from grounding, collision or weapon effects.

They also have good efficiency over the required speed range because they are effective in recovering a good part of the ship's frictional drag by ingesting the low momentum boundary layer at the waterjet

inlet and have been shown to produce a negative thrust deduction with the use of flush-mounted inlets. In addition, they offer improved maneuverability because they can vector gross thrust rather than net thrust to great advantage and can use buckets out of the slip stream for reverse thrust to reduce stopping distance and avoid the need to reverse shaft rotation or have the complication and expense of reversible pitch blades. Also, waterjet impeller speeds of rotation are generally higher than with marine screws which leads to lower power transmission weight. The only possible issues for some applications are (1) the signal left behind by the jet wake compared to the wake from submerged marine screws, and (2) the periodic change in engine torque loading if air ingestion were to occur in very rough water.

## 1.2. So Why Axial-Flow Waterjet Pumps?

As mentioned earlier, high ship speeds generally require the use of slender hullforms (to reduce the ship's wave drag) and efficient, but compact, propulsion systems (to minimize the total installed power and installation space required). However, today's commercially available large waterjets above 10,000 horsepower are large mixed-flow pumps. Figure 2 is a simple illustration of the size comparison. It shows that, for the same inlet diameter and thus the same unit thrust, the transom flange of the axial-flow pump can be at least 33% smaller and thus allows 3 axial-flow pumps to occupy the space needed by 2 mixed-flow pumps. Therefore, the use of 3 axial-flow pumps instead of 2 mixed-flow pumps can provide up to 50% more thrust from the same transom or, conversely, for the same total thrust, the use of axial-flow pumps can allow for a significantly reduced transom size and thus a significant reduction in wave drag for a high-speed ship.

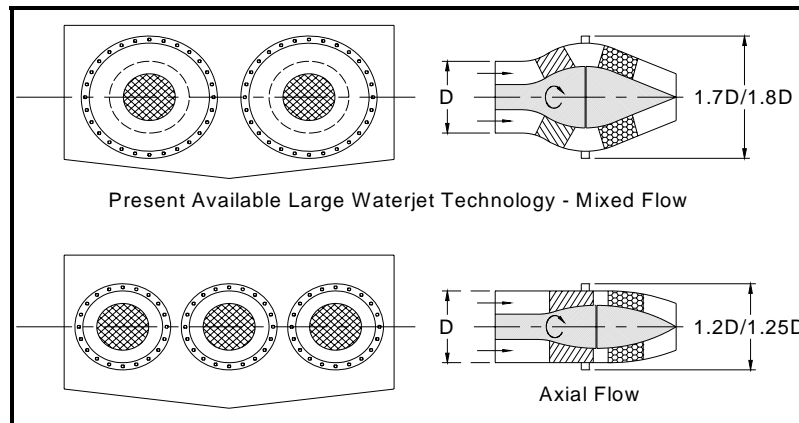


Figure 2: Pump size comparison

## 2. The Development Program

Axial-flow waterjet pumps are not new. They have been in serious use in various forms for several hundred years, *Allison (1992)*. The type of axial-flow pump selected for this current application has its roots in separate work performed originally by Aerojet General Corporation and by Rocketdyne in the U.S. when ship speed was once before popular with the U.S. military. This occurred in the 1960's and 70's, but was subsequently discontinued. The largest axial-flow pumps then built were the 19,000 hp Aerojet pumps for the PHM hydrofoil and the 40,000 hp Rocketdyne axial-flow pumps for the 3K SES which were under construction when the program was cancelled in 1978.

However, starting in 1987, Band, Lavis & Associates (BLA, now CDI Marine Systems Development Division (CDIM-SDD)) picked up the thread and began further development that has now resulted, over the last 18 years, in numerous pump model tests for the world's leading waterjet manufacturers and installation on several craft, including the U.S. Marine Corps Expeditionary Fighting Vehicle (EFV, formerly the AAV) high-speed tracked amphibian. Also, starting in 1996, BLA received a

major boost in funding from DARPA and later significant research funding from the University of New Orleans to investigate hull-inlet interactions. This was followed by major funding from CCDoTT (The Center for Commercial Deployment of Transportation Technologies) out of California State University at Long Beach for the work which is the major subject of this paper. Significant support was also provided to the U.S. Navy's High-Speed Sealift Program for which BLA recommended compact axial-flow waterjet development and prepared a comprehensive Technology Development Plan (NSWCCD 2002). Based on these recommendations and separate recommendations made to NAVSEA PEO Ships, the Office of Naval Research (ONR) launched a new program in 2006 for industry to develop high-power compact waterjet propulsion systems for current and future military applications.

The work reported in this current paper is the most recent effort in this evolution. It started in 2002 when CCDoTT funded BLA (CDIM-SDD) for a 4-year, 4-phase program to examine technology options and eventually perform RDT&E to develop and validate compact axial-flow pumps for waterjets. The paper focuses on describing Phases 3 & 4, while Phases 1 & 2 are described in more detail on the CCDoTT Website at [www.ccdott.org](http://www.ccdott.org) and in *Lavis et al. (2006)*. The 4 phases of the project were as follows:

**Phase 1**, completed in August 2002, studied options for compact units, including the following: 1) Pumps with Contra-Rotating Blade Rows, 2) Pumps with Inlet Pre-Swirl Vanes, 3) Ventilated Pumps, 4) Super-Cavitating Pumps, and 5) Axial-Flow Pumps. The latter was chosen for further work.

**Phase 2**, completed in September 2003, developed the concept design of a waterjet-propelled, 50-knot, 600-ft long RO/RO ship for commercial coastal short-sea shipping. This design was developed with help from the CDIM-SDD whole-ship design synthesis model ComPASS™, which helped to confirm the choice of axial waterjet pumps as having the most favorable ship impact to minimize ship fuel consumption and maximize overall ship economy of operation. We then developed the detailed hydrodynamic design of the pump for this ship using the inverse potential-flow code TURBODesign<sup>-1</sup> and the Navier Stokes solver CFX.

**Phase 3**, completed in July 2005, involved the Computational Fluid Dynamic (CFD) analysis, manufacture, and tunnel testing of a model waterjet pump that was required to adequately validate the pump's critical powering characteristics and cavitation limits.

**Phase 4**, to be completed in October 2006, involved the construction and testing in a towing tank of a suitable high-speed model for, among other things, the critical interaction effects between the hull and the waterjet inlet. It determined the pump's powering characteristics at design point and off-design operating conditions. The whole-ship and ship interaction data, combined with pump model tests of Phase 3, provided the critical information necessary to validate the design process and the CFD modeling process. This enabled realization of the Overall Project Goal: To enable the realistic design and prediction of overall full-scale performance of large (>40 MW) axial-flow pumps in a high-speed ship application using the proper and appropriate model testing and data scaling procedures such as those defined by the International Towing Tank Conference (ITTC 2002).

### 3. Phase-2, Ship Design and Waterjet Pump Requirements

In developing a ship concept design and the detail hydrodynamic design of a pump in Phase 2 of the CCDoTT work, we chose as a mission one of 15 missions explored by the Fast Sea Lift Innovation Cell at NSWC Carderock (NSWCCD May 2002). This mission was one recommended by MARAD as a Short-Sea Shipping Mission having both commercial and military application. For the design of the ship, we used our whole-ship design synthesis tool ComPASS™ that not only allowed us to select the least cost choice of hull type, but also helped us to select between mixed-flow and axial-flow pumps and an initial characterization of performance and size required.

The selected vessel is shown in Figure 3 relative to the rest of the 4-dimensional design space. Here, displacement is shown plotted as a function of ship length and ship length-to-beam ratio with the shading on the chart showing ship life-cycle cost per hour of operation. A beam-to-draft ratio above 2.5 was desired to achieve a reasonably low draft, so a least cost solution was found having a length of 600 ft and a displacement of 8376 LT. This ship was propelled by four 90-inch diameter axial-flow waterjets, each absorbing 57,330 hp. This ship design was then used as the basis for setting the requirements for, and design of, the axial-flow pump described in the paper. This pump could easily be scaled to meet other powers and ship speed requirements currently being explored by the U.S. military.

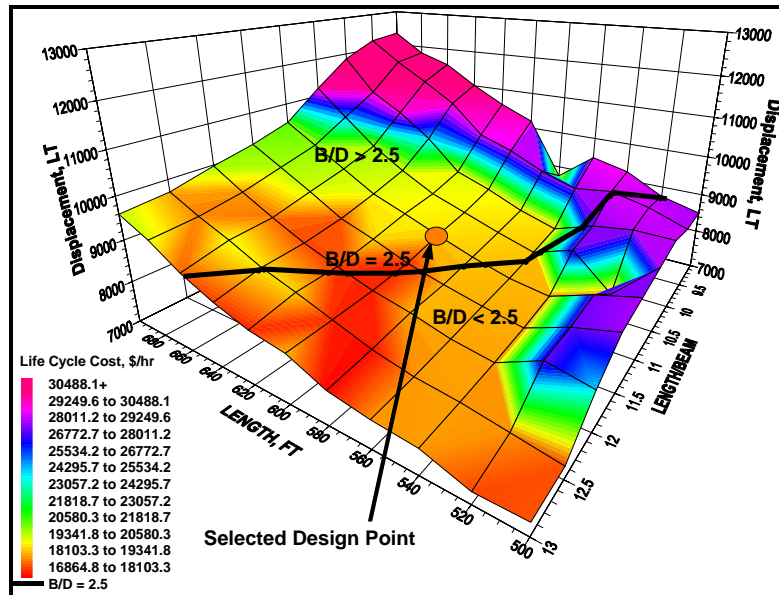


Figure 3: ComPASS™ results for propulsion with axial-flow waterjets

## 4. Waterjet Propulsion System Design

### 4.1. Pump Geometry

TURBOdesign<sup>-1</sup> was used to develop the detailed geometry of the rotor blades using the meridional geometry, radial loading distribution, and blade numbers based on initial development using a streamline curvature method. TURBOdesign<sup>-1</sup> is a potential-flow inverse method where the requirements for the rotor are inputs and the blade geometry is the output. TURBOdesign<sup>-1</sup> does not take into account the viscous effects, but these effects were modeled using the CFD Navier-Stokes solver ANSYS CFX. TURBOdesign<sup>-1</sup> and ANSYS CFX were used iteratively to arrive at the final optimized rotor blade geometry. The blade profile used for the resulting 90-inch diameter, 5-bladed impeller rotor was a modified C4 section with a 6.67 percent trailing edge thickness. The rotor hub axial length was 58.5 inches with a maximum normal blade thickness of 3.937 inches, and the tip axial length, which was leaned forward 1.75 inches, was 60.25 inches with a maximum normal blade thickness of 2 inches. Figure 4 shows the 3-dimensional geometry with the blade surface static pressure distribution on the leading edge suction side where the pressure would be the lowest. This shows that the minimum pressure is 21.56 kPa, or 7 feet of seawater margin above vapor pressure at the 41-knot minimum full-power speed of the 50-knot design top speed application.

Structural Finite Element Analysis was next carried out to check blade strength to resist the loadings defined by TURBOdesign<sup>-1</sup> and the centrifugal loads for a speed in excess of the design speed (Figure 5). Deflections were also checked to ensure that the blades would not contact the housing under load.

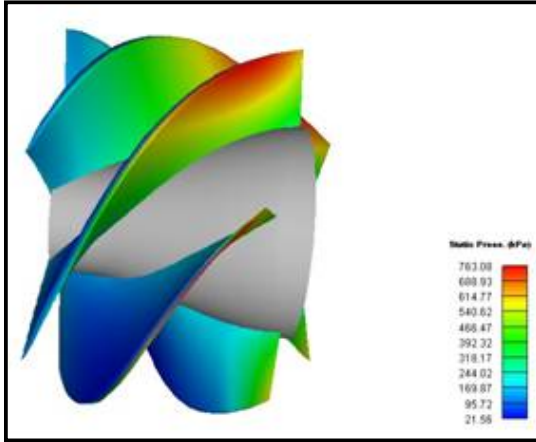


Figure 4: Blade surface static pressure distribution for pump rotor

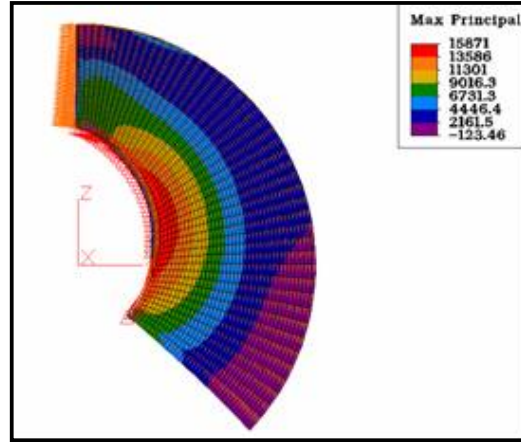


Figure 5: Contour plot of stress for the waterjet rotor blade

#### 4.2. Inlet Geometry

Another challenge is good waterjet inlet design. Here, the objective is to design to capture as much of the ship's lower momentum boundary layer as possible with minimum inlet loss, favorable pressure gradients, and no areas of very low pressure particularly over the upper suction surface of the inlet that could cause separation and vapor cavities that block flow. For this, we again used ANSYS CFX and proceeded through a range of design geometries to seek a preferred solution. Figure 6 illustrates some of the results in which inlet ramp angles varied from 32 to 26 degrees with progressive reduction in the extent of lower pressure indicated by the color blue. Further detail on inlet design as well as nozzle design can be found in *Lavis et al. (2006)*.

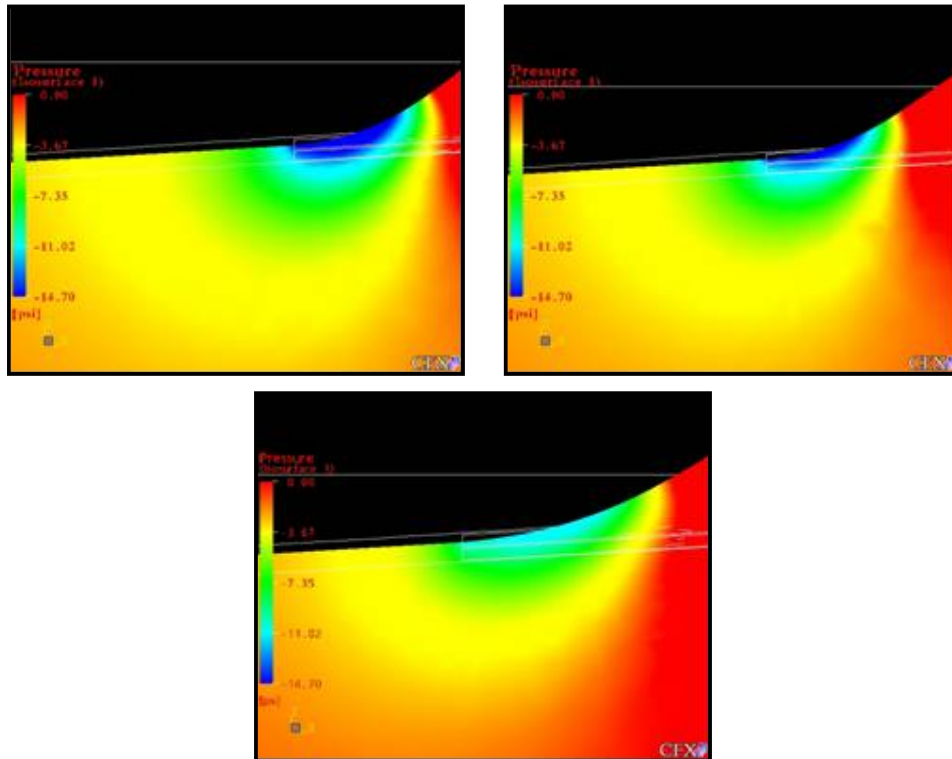


Figure 6: Ramp tangency static pressure distribution with ramp angles of 32, 28 & 26 degrees

## 5. Prediction of Performance and Cavitation Limits

The cavitation margin was set at 1.2 for a craft speed of 41 knots, which is 1.2 times the net positive suction head (NPSH) at complete pump head breakdown. This cavitation margin allows the waterjet to absorb full installed power at 41 knots for acceleration to full speed and enhances off-design performance. The inlet ram recovery is the percentage of the dynamic pressure at the pump face that remains from the amount that was in the inlet capture stream tube. The ram recovery is calculated from an empirical relationship that is a function of inlet velocity ratio, IVR, which is the ratio of average velocity at the pump face to the average velocity in the inlet capture stream tube. The ratio of the jet velocity from the nozzle to the ship speed is known as the jet velocity ratio (JVR). For a sealift-type case, it was determined that a pump diameter of 90 inches would best meet cavitation and performance requirements for the 57,330 shaft horsepower. The jet velocity ratio (JVR) for this requirement is 1.56. A JVR in this range tends to provide the optimum balance between propulsive efficiency and unit size and weight.

The waterjet pump performance can be calculated from the ANSYS CFX calculations by summing up the tangential force on the rotor blade surface times their radius to calculate the required torque of the pump at the design RPM. The hydraulic power is calculated by taking the mass flow rate times the rise in total pressure across the pump. The pump hydraulic efficiency is the pump hydraulic power divided by the shaft power. The optimized pump was predicted to produce 4 percent more headrise at the design flow rate. Figure 7 shows the calculated performance in comparison to test measurements. The initial assumed design value for hydraulic efficiency of 90% was exceeded by 2.9% for the optimized pump. This higher efficiency can be used to push the ship faster using the 57,330 horsepower available, or represents a savings in fuel since less power will be needed to push the ship at 50 knots.

As a result of the CFD analysis of the overall design, several improvements to the initial design criteria were established. The inlet ram recovery was higher than original empirical expectations. The large size of the waterjet inlet reduces its surface to volume ratio, which minimized frictional losses and improved the ram recovery from about 85 percent to near 90 percent. Increased ram recovery reduced the head rise requirements of the pump to operate at a given JVR and improved cavitation margins for the pump by increasing the NPSH. Stress analysis of the blading for the full-scale waterjet impeller and stator showed that stresses were well within reasonable limits for this design.

## 6. Pump Performance and Cavitation Tests

The water-tunnel testing of a 7.5-inch diameter pump, or 1/12<sup>th</sup>-scale model, of the advanced axial-flow waterjet pump was performed in the spring of 2005. Proper model testing requires proper construction of the model components, which requires special attention to details and quality machining. The water-tunnel testing was performed at the Carderock Division, Naval Surface Warfare Center (CDNSWC) in West Bethesda, MD, using the 24-inch water-tunnel facility. The water-tunnel pump model testing examined the performance and cavitation characteristics of a scaled axial-flow waterjet pump. The water-tunnel testing allows the basic full-scale pump performance to be evaluated from the use of the appropriately scaled model. Figure 10 of this technical paper shows a photo of the instrumented model axial pump assembly installed in the water tunnel and ready for testing. The water-tunnel testing allows the pump to be tested separately from the remainder of the waterjet system to determine its performance. Later self-propulsion tests of a suitable hull model with scaled waterjet inlets can then be conducted and later combined with the pump performance results to determine the overall waterjet system performance for the full-scale ship.

Model design point parameters:

Impeller diameter:	7.50 inch	Maximum power:	50 shp
Nozzle diameter (unblocked):	4.87 inch	Flow rate (target):	8.35 cfs
Shaft speed (target):	2440 RPM	Headrise (target):	56 ft freshwater
Shaft speed (acceptable):	2000 RPM	Suction specific speed (design point):	12,730

Figure 7 shows the model test pump components and assembly. The water tunnel had a rear drive system, and the waterjet nozzle area was adjusted to account for the drive shaft blockage.

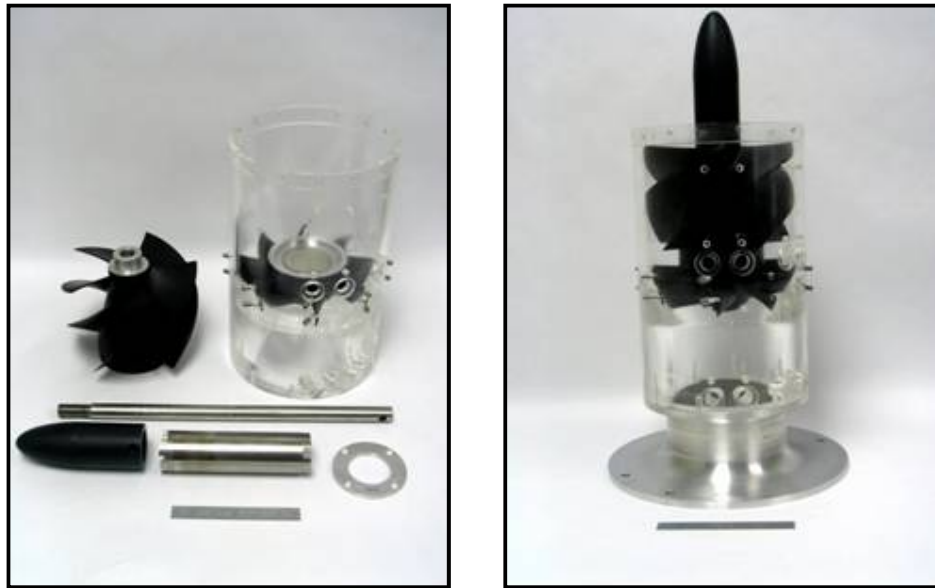


Figure 7: Model pump components & assembly

Performance runs were made to ultimately establish the head-flow characteristics of the pump as well as its power requirements and hydraulic efficiency. These tests were run over a range of flows at different pump rotational speeds so that design and off-design conditions were covered. Various flow rates through the pump could be set by use of the tunnel circulation pump and/or additional flow resistance rods installed downstream of the pump exit nozzle. During the performance runs, multiple wall differential static pressure measurements were taken at locations between the pump inlet location and the rotor/stator gap and the nozzle throat. The wall static pressure differential gave information on the change in wall static pressures between locations and was supplemented with data from LDV surveys and Kiel probe data to generate the representative head-flow curve. All this data additionally determined the effective horsepower transmitted into the water by the pump impeller and what remains at the nozzle section so that rotor efficiency and overall pump hydraulic efficiency could be obtained at the various operating conditions. Figure 8 shows model performance data at 2000 rpm compared with initial CFD predictions for the model pump setup. The water-tunnel drive motor was set up to measure the water-tunnel drive shaft torque. Corrections to torque were made to account for initial instrumentation offsets and drive system torque losses up to the pump using the tare test results. The resulting corrected torque values were the values of torque required to drive the pump rotor at its various test conditions.



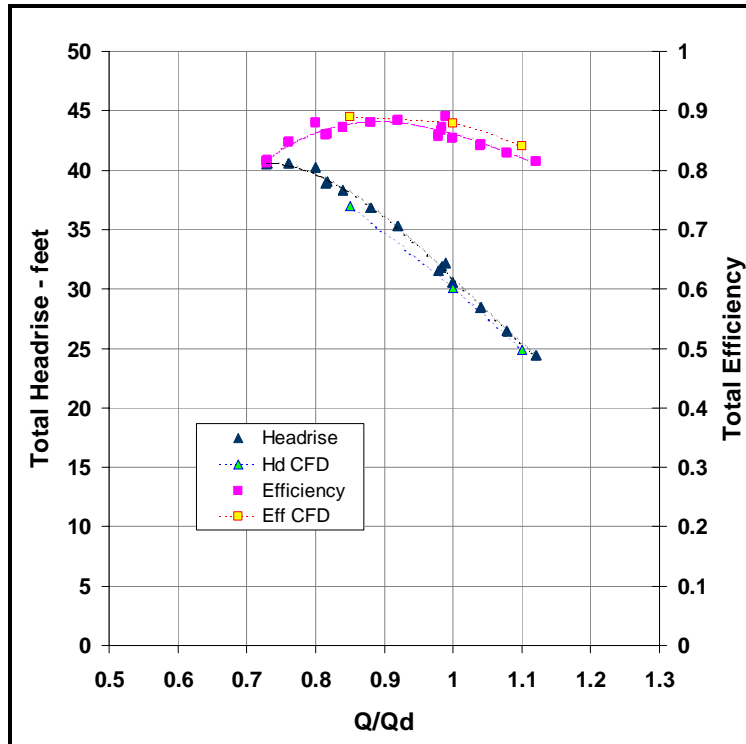


Figure 8: Performance with the nozzle static profile at 2000 rpm

Cavitation runs were made to determine the likely cavitation performance of the pump. During the cavitation runs, the tunnel pressure was changed to control the Net Positive Suction Head (NPSH) in front of the pump inlet face, where NPSH is the total pressure above vapor pressure at that location. The cavitation runs were performed at a test pump speed of 2000 rpm. The pump was mounted inside a clear acrylic shroud which enabled viewing of the impeller and stator blade rows as well as the nozzle section. By use of a strobe light, the rotating pump impeller could be made to appear as though it was standing still in order to observe any occurrences of cavitation in the impeller. In this manner, as the tunnel pressure was lowered sufficiently to initiate cavitation, the cavitation anywhere in the pump could be observed as to type, location and extent.

The presence of cavitation does not necessarily degrade performance, as a pump can operate with some amount of cavitation present. This is not desirable on a continuous basis, but is acceptable for transient operation such as during periods of ship forward acceleration. When the amount of cavitation present becomes excessive, the pump can no longer maintain its headrise and the pump enters cavitation breakdown where the headrise begins to fall off, usually in a dramatic form with any further decrease in NPSH. Cavitation breakdown is normally classified as the point where there is a 3% reduction in the pump total headrise from its noncavitating condition. Cavitation runs were made with decreasing NPSH until breakdown occurred, then the NPSH was increased to measure the recovery from breakdown and to determine any hysteresis effects. Another term used for cavitation analysis is Suction Specific Speed ( $N_{ss}$ ).  $N_{ss}$  is defined by:

$$N_{ss} = \frac{RPM * GPM^{1/2}}{NPSH^{3/4}} \quad [1]$$

$N_{ss}$  is a dimensionless term, but it is used with more convenient pump terms such as RPM and GPM which makes it appear otherwise, but, since these terms only vary by a constant from the true dimensionless form, the  $N_{ss}$  term functions as a dimensionless term. The  $N_{ss}$  equation is important

for scaling the model data to full scale since Nss performance at model scale will translate to the full-scale performance. Design point Nss for the full-scale design is about 12,500. The pump can operate at Nss values above this to provide for cavitation margins and better off-design performance, but operation at the further elevated Nss should be kept to short periods, such as acceleration, as the increased potential presence of cavitation can damage the pump, although it may not affect performance until the breakdown Nss is reached. Design of a pump to operate properly with a high Nss of 12,500 or greater requires significant attention to the design detail. The use of CFD in the analysis has been a critical step in developing a high-performance design.

Figure 9 shows the cavitation run where the NPSH was changed in increments by adjustment of the tunnel pressure at the model design flow rate. The head ratio,  $H/H_0$ , was the wall static pressure difference across the pump divided by the initial static pressure difference across the pump at the beginning of the test with a high NPSH value and no cavitation present. As the NPSH was reduced, the head ratio remained essentially constant at a value of 1 until a critical value of NPSH was reached, at which point a temporary increase in head ratio occurred prior to the collapse of the head ratio, which would indicate cavitation breakdown. This temporary increase in head ratio just prior to the breakdown region is not uncommon in cavitation testing and has been attributed to the existence of improved flow geometry due to a modest amount of cavitation. The second photo of Figure 10 shows the cavitation for the design flow case. Review of the photo indicates that the main source or type of cavitation that occurred was tip leakage cavitation. There is a pressure difference between the pressure and suction side of the blade. This pressure difference causes flow to accelerate through the tip gap between the rotating blade tip and the surrounding stationary shroud. Some flow through the gap is beneficial, but an increase in pressure difference across the gap, combined with the local pressure conditions, can cause the flow accelerating through the gap to drop the local static pressure below the vapor pressure, which results in the formation of a jet of vapor. The photos also indicate that the tip leakage was not always uniform from blade to blade at different Nss values. This was most likely due to tip clearance variations from blade to blade. Although every attempt was made to center the impeller in the shroud, the small scale of the model, the final component assembly after the gap is set, and operating loads inevitably caused some minor variations in the gap.

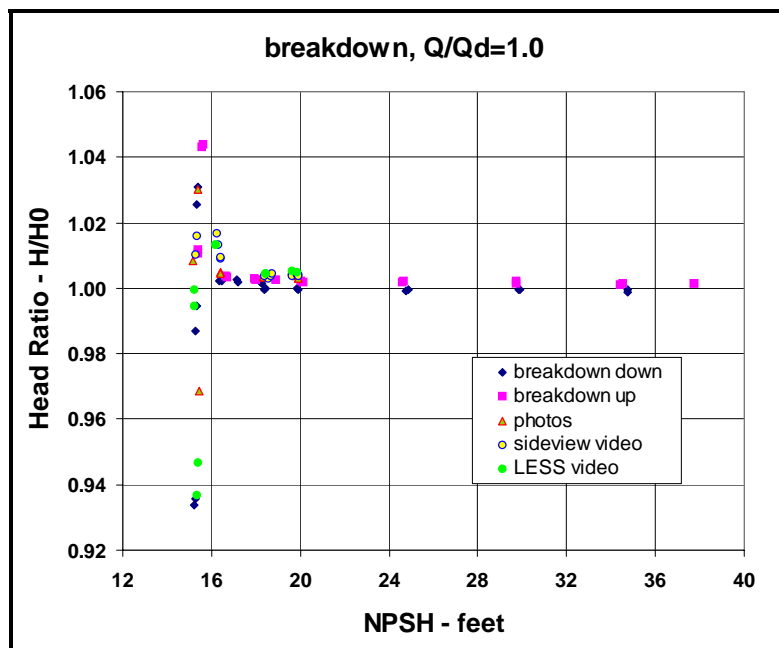


Figure 9: Cavitation breakdown runs at  $Q/Q_d = 1.0$  and 2000 rpm

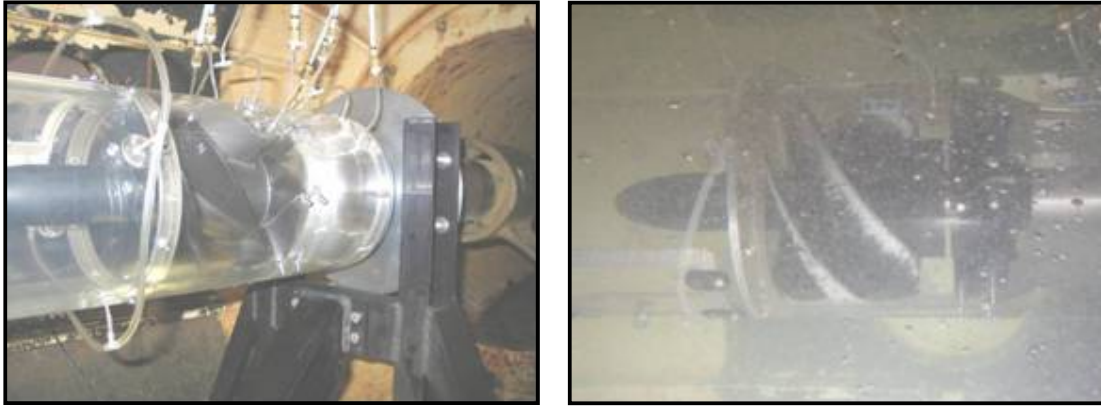


Figure 10: Cavitation run at 2000 rpm and  $Q/Q_d = 1.0$

The tip leakage cavitation can be controlled to some extent to allow operation of the full-scale pump at higher  $N_{ss}$  values. Better control of the tip clearance to optimum minimum values will delay the onset of cavitation. Also, the model pump had sharp corners at the impeller tip section. Putting a small radius on the pressure side tip section will enable a more gradual acceleration of flow through the tip gap instead of the abrupt acceleration caused by the square edge arrangement. This would help push the tip leakage cavitation inception to somewhat higher  $N_{ss}$  values. In addition, the model likely experienced a higher differential pressure across the tip gap due to an increased amount of boundary layer flow that was present at the pump face from the test setup. The photos of Figure 10 indicate that the impeller leading edge is not a source of cavitation and there is no indication of cavitation problems in the stator or nozzle region. The S-bend in the shroud wall shortly after the stator exit is a typical low-pressure region, but did not show any indication of vapor formation.

## 7. Self-Propelled Model Tests

Self-propulsion model testing of a single representative large catamaran-type side-hull with a pair of operating scaled waterjet inlets was undertaken. Since the main point of interest in these tests is to look at and determine the interaction-type effects between the hull and waterjet inlet, only a single hull was used for the testing to reduce complexity and consequently the overall expenses. Testing was performed at the Naval Surface Warfare Center, Carderock Division, on the Towing Tank Carriage No 1. The 17.5-to-1 scale self-propulsion model size built was 19.8 feet long, which is of sufficient size to provide accurate data based on the experience of the towing tank engineers. The model included operating scaled waterjet inlets with representative waterjet pumps. For the self-propulsion testing, it is important that waterjet inlets operate at scaled flow rate so that the inlet-hull interactions are modeled for their effects on overall propulsive performance. The waterjet pumps are not specifically modeled since, at this model-scale ratio, the Froude-scaled testing conditions prevent pump model operation at cavitation and Reynolds numbers that can approximate full-scale values for these critical parameters. The model axial pumps will move the proper flow rates and will be representative of the full-scale waterjet pump, but because the blade thickness becomes too thin to scale at model scale, the blades were given constant thickness and built on the representative axial pump camber surface. The waterjet pump included both an impeller and a stator blade row with a scaled nozzle for the arrangement. Rapid prototyping was used to fabricate the model inlets and the model pumps. This allows accurate components to be made rather quickly and at reasonable cost compared to any other possible alternatives. At the model-scale requirements, stresses and loads are within the capability of available rapid prototyping material, which is a form of nylon-based material. The hull is symmetrical about the hull centerline so that everything forward of the waterjet inlets would be the same, but mirror-imaged, about the hull centerline. The hull has a pair of waterjet inlets at the stern that are also mirror images of each other about the hull centerline. Using two representative axial-flow pumps with opposite rotation to each other would then represent a mirroring of the pumps about the hull centerline. Since the model tests were conducted in a straight-ahead

condition, both pumps would be expected to have identical performance. This allows for full instrumentation and measurements on one pump to be indicative of what is happening on the other pump, with some measurements taken on the second pump to assure consistency. Separate water-tunnel testing of larger-scale axial pump models was previously performed to adequately define critical powering characteristics and cavitation limits of the waterjet pump design. The extrapolated data obtained in both water-tunnel and towed model tests then constitutes a complete data set characterizing the overall performance of the combined hull and propulsor.

CDIM-SDD has conducted extensive advanced axial-flow waterjet propulsion work over a period of 18 years, and the current self-propelled model tests represent the completion of a 4-phase program for CCDoTT. The overall objective of this final phase of work was to test a self-propelled model (Figure 11) in a towing tank to completely define the hydrodynamic performance characteristics of a compact axial-flow waterjet propulsor in a representative high-speed ship. Measurements were made to verify design predictions, provide off-design performance information, and yield flow-field data for use in understanding the behavior of the propulsion system design as installed in the hull model. These tests have just been completed and numerical results were, unfortunately, not available in time to meet the publication date for this paper. Data will ultimately be scaled to the full-scale ship design used for the model, using the waterjet design which was water-tunnel model tested, and that data combined with this self-propulsion model will be used to predict performance of an operational system at full scale. Towing tank tests of waterjet propulsors and ship hulls present a unique challenge to engineers and experimenters because of interaction effects normally absent, or of far less importance, in marine-screw propeller installations. The great body of towed model test data and experience with open propeller designs has resulted in a generally high degree of confidence in predicting full-scale performance. Waterjet hull model testing is relatively new, and the body of test data and testing experience is a small fraction of the propeller database. For these reasons, the fundamentals of waterjet model testing have been the subject of a great deal of attention and study in recent years. The development of the momentum flux method of estimating powering characteristics and interaction effects has allowed model testing to be performed with better confidence than previously, and the database is expanding slowly but steadily. While the overall waterjet characterization capabilities remain somewhat limited relative to open water and towed model propeller testing, prediction techniques are improving. The development of a database with a significant quantity of model to full-scale data correlations is a matter of great importance in improving levels of confidence in predicting waterjet system performance for advanced high-speed ships.



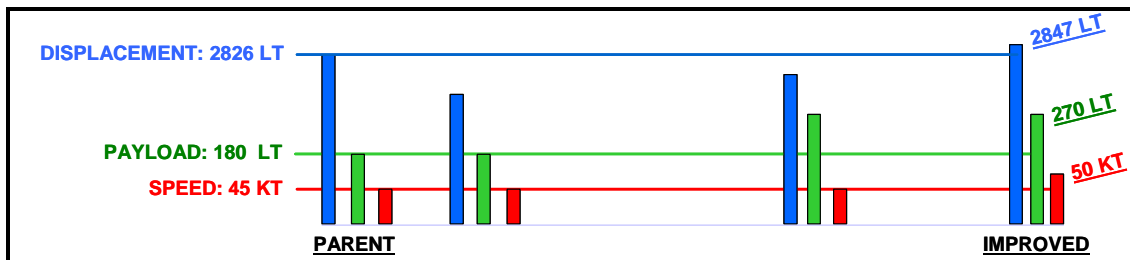
Figure 11: Self-Propulsion Model in the Towing Tank

## 8. Whole-Ship Impact of Compact Waterjet Propulsion

In Chapter 3, it was stated that the developed pump could easily be scaled to meet other high-speed ship requirements currently being explored by the U.S. Military. Table I summarizes the result of a study that used COMPASS™ to design an LCS-type monohull, referred to as the “Parent Ship”, that was propelled by mixed-flow pumps, as characterized in column 1, and compared this ship with another designed with axial-flow pumps, characterized in the subsequent columns of Table I. The parent LCS has a displacement of 2826 LT and is capable of carrying a military cargo of 180 LT at a speed of 45 knots for a range of 1500 NM. By changing to axial-flow pumps, a major change occurs as shown in column 2. Displacement is reduced by 250 LT and power required falls by 10,000 SHP for the same speed and range capability. To take advantage of this, we increased the cargo by 50%, from 180 LT to 270 LT, to give the results shown in columns 4 & 5, for which the displacement increased to 2785 LT with 270 LT of cargo while keeping the same speed and range with the same installed power. Since this design was still 101 LT lighter than the parent, it was possible then to take even further advantage of the change by increasing the ship’s speed from 45 to 50 knots. In this case, as shown in the last two columns of Table I, the ship’s displacement increased to 2847 LT, which is only 21 tons greater than the displacement of the parent, while the propulsion power required increased to 70,000 SHP, which is only 3000 SHP greater than the parent and considered to be within the capability of the original power plant. Thus, by taking advantage of all the synergies afforded by this single change in propulsor type, including weight saved with a smaller, higher speed pump on a smaller transom with less drag, the military cargo was increased by 50% and the ship’s speeds increased by 5 knots. Note that the full effect of these synergies would not occur by simply back fitting a different pump to an existing ship. Clearly, the advantage of such a choice taken early in the design process is significant.

Table 1: The Synergistic Whole-Ship Impact of Compact Pumps

Change from Mixed Flow WaterJet to Advanced Compact (Custom) Axial Flow WJ Propulsor								
	Parent Ship	Change Propulsor		Increase Cargo 50%			Increase Speed to 50kts	
Propulsion	Mixed Flow WJ	ACWJ	Compared w/Parent		ACWJ	Compared w/Parent		Compared w/Parent
Displacement (LT)	2,826	<b>2,576</b>	-250		<b>2,785</b>	<b>-101</b>	2,847	21
Cargo (LT)	180	180		<b>+90</b>	<b>270</b>	<b>+90</b>	270	<b>+90</b>
Power (Gas Turb) (SHP)	67,000	<b>57,000</b>	-10,000	<b>Installed</b>	67,000		<b>70,000</b>	<b>3,000</b>
Power (Diesel) (SHP)	8,700	8,700			8,700			
Speed	45	45			45		<b>50</b>	<b>5</b>
Range	1,500	1,500			1,500		1,500	



## 9. Conclusions

The paper has demonstrated that the compact axial-flow waterjet pump has excellent overall hydrodynamic and cavitation characteristics. Performance of the pump is basically in agreement with initial CFD predictions, although some differences between the CFD pump model details and the actual test setup are responsible for certain variations. Overall, headrise was slightly higher than expected, but this is likely due to the thick duct wall boundary layer flow region upstream of the model impeller. Efficiencies were slightly lower than CFD predictions, but the differences between the CFD arrangement and the model test geometries are deemed likely to account for most of the variation. Further analyses would be incorporated into the development and adaptation of the compact axial-flow pump design as a matter of course to refine the design.

So, our progress to date from the use of a combination of advanced CFD codes and model tests has seen: (1) the elimination of the need for the inducer stage from earlier axial waterjet designs, which has clearly simplified the pump as well as reduced its overall length, weight and cost of manufacture, (2) the use of an inverse potential flow code and the CFX Navier Stokes Solver to significantly improve pump efficiency and cavitation performance. In addition, from our current tests, we will improve our understanding of hull/waterjet inlet interactions.

Thus, in summary, we have recognized an important need and we have brought to the community a viable solution. We have demonstrated the advantages of axial-flow waterjet pumps via extensive test and analysis. Advantages include significant size and weight savings for the same duty compared to mixed-flow designs. This, in turn, allows the use of slender transoms leading to less ship resistance. Pumps having higher rotational speeds results in better power density for the pump and power transmission along with performance less limited by cavitation. The paper has also shown, by example, that the synergistic whole-ship impact of using these compact pumps is significant in terms of potential improvements in ship speed and payload.

We have also assembled the best advanced tools for design and, in doing so, have significantly advanced the state-of-the-art and have encouraged our Navy to invest for transition to meet current and future needs. The overall program is, therefore, considered to be an outstanding success with the potential of having far-reaching benefits to future high-speed ships.

## 10. Acknowledgements

Assisting CDIM-SDD in Severna Park, MD, on this project for CCDoTT has been the Naval Surface Warfare Center, Carderock, MD (NSWCCD), Marine Propulsors Company, Berlin, MD (MPC), and the Office of Naval Research (ONR).

Specific individuals that have made significant contributions to this 4-year program of work, and for which we are very grateful, have included: Alan Becnel (CDIM-SDD and NSWCCD); John Stricker (MPC); Scott Gowing; John Hoyt (NSWCCD); Jeff Benson, Diane King and Bill Baker (CDIM-SDD); Stan Wheatley and Steve Hinds (CCDoTT); Dan Sheridan (Noesis); and Dr. Ki-Han Kim and Dr. Paul Rispin (ONR).

## 11. Nomenclature

<b><u>Symbol</u></b>	<b><u>Definition</u></b>	<b><u>Units</u></b>
B	Ship's Waterline Beam	ft
CFD	Computational Fluid Dynamics	--
Circle K	$0.468 (V / W^{1/6})$	--
Circle Q	$P / (VW)$	--
D	Pump Inlet Diameter or Ship's Draft	ft

GPM	Gallons per Minute	gal/min
H	Headrise	ft
H0	Initial Headrise	ft
IVR	Inlet Velocity Ratio	--
JVR	Jet Velocity Ratio	--
NPSH	Net Positive Suction Head	--
N <sub>ss</sub>	Suction Specific Speed	--
P	Power Required for Maximum Speed	ft.lb/sec
Q	Volume Flow Rate	ft <sup>3</sup> /sec (cfs)
Q <sub>d</sub>	Design Point Volume Flow Rate at Design RPM	ft <sup>3</sup> /sec
RPM	Shaft Rotational Speed	revs/min
shp	Shaft Horsepower	horsepower
V	Ship's Maximum Speed in Calm Water	ft/sec
W	Ship's Full Load Displacement	lb

## 11. References

Hoyt, J. (2002): "Transport Factor" Data for a Range of Ship Types", NSWCCD, February.

Allison, J.L.(1993): "Marine Waterjet Propulsion" *Transactions* of SNAME, 101

NSWCCD-20-TR-2002/06 (2002): "High-Speed Sealift Technology Development Plan", May.

Lavis, D.R., Forstell, B.G., Purnell, J.G. (2006): "Advanced Compact Waterjet Propulsion for High-Speed Ships", IMDC Ann Arbor, Michigan, May.

ITTC Proceedings – VOLUME II (2002): "The Specialist Committee on Validation of Waterjet Test Procedures." Final Report and Recommendations to the 23<sup>rd</sup> ITTC, p 387-415, p 709-711